

An Investigation and Computational study of an amino acid as Corrosion Inhibitor for Stainless steel in acidic medium

M. Kalpana Devi^{1,2}, Felicia Rajammal Selvarani²

¹ P.G. and Research Department of Chemistry, Bishop Heber College (Autonomous),
Tiruchirappalli - 620017(INDIA).

² P.G. and Research Department of Chemistry, Holy Cross College, (Autonomous),
Tiruchirappalli - 620002(INDIA).

Email id:- kalpana.devi2008@gmail.com

Abstract

The corrosion inhibition of L-Glutamic acid for stainless steel in HCl solution has been calculated by weight loss study. It is found that the inhibition efficiency of L-Glutamic acid (LG) increases with increase in the concentration. The inhibition efficiency of LG decreases with increase in the temperature. Three adsorption isotherms are tested; out of which the El-Awady et al adsorption isotherm model fits well. The free energy of adsorption (ΔG^0_{ads}) suggests that adsorption is a spontaneous physisorption process. SEM and EDX confirm the formation of protective film on the stainless steel surface. The quantum chemical parameters show a good correlation between the experimentally calculated inhibition efficiency and theoretical inhibition efficiency.

Key words: L-Glutamic acid, El-Awady et al adsorption isotherm, SEM and EDX

1. INTRODUCTION

Corrosion is the destruction of metal by the chemical attack. It is a constant and incessant problem, often difficult to eliminate entirely. But prevention would be more practical and doable than complete elimination [1,2]. The addition of an inhibitor is necessary to prevent corrosion i.e. to reduce the dissolution of metals in these acidic environments [3,4]. Corrosion inhibitors play a vital role in corrosion deterrence in many industries. Inhibitors are substance which when added in small quantity to a corrosive environment, lower the corrosion rate.

In the present study L-Glutamic acid is used as an inhibitor to prevent the corrosion of stainless steel in acidic medium. Glutamic acid is often used as a food additives and flavour enhancer in the form of its salt, known as monosodium glutamate (MSG). Glutamate also plays an important role in the body's disposal of excess or waste nitrogen. L-glutamic acid

has amino group ($-NH_2$) and carboxyl group ($-COOH$). These groups can coordinate with metal through the nitrogen atom of amino group and oxygen atom of the carboxyl group to reduce the corrosion [5,6]. The aim of this work is to study the effectiveness of L-Glutamic acid as a corrosion inhibitor for stainless steel in 1.0 M HCl solution.

2. MATERIALS AND METHODS

2.1 Preparation of the stainless steel specimens

The composition of the stainless steel is as follows 0.12% of C, 1.00% of Si, 1.00% of Mn, 16.00% of Cr, 0.75% of Ni, 0.04% of P, 0.03% of S and balance Fe. Stainless steel specimens of the dimensions 4.5 cm×1.5 cm×0.04 cm and containing a small hole of about 2mm diameter near the upper edge

are taken. Specimens are polished to mirror finish, degreased with acetone and used for mass-loss and surface analysis.

2.2 Mass-loss Method

A rectangular stainless steel specimen of area $4.5\text{ cm} \times 1.5\text{ cm} \times 0.04\text{ cm}$ having a small hole of about 2 mm diameter near one end is used. The specimen of the metal is polished using different grades of emery papers to give a mirror like finish. It is degreased by immersion in acetone, washed with distilled water and dried. All the weighing of the stainless steel specimens are carried out using Shimadzu Ay 220 model electronic digital balance with sensitivity of 0.1 mg in 220g range. The weighed specimens are suspended by glass hooks in 100 mL beaker containing 100 mL of various test solutions. After 1 hour of immersion, the specimens are taken out, washed in water dried and weighed. From the weight loss data, corrosion rates and percent inhibition efficiencies (IE %) are calculated.

2.3 Surface Morphology analysis Scanning Electron Microscopy

The stainless steel specimen is cut in to small pieces with a dimension of $2\text{ cm} \times 1\text{ cm} \times 0.04\text{ cm}$. The pieces are suspended in the best concentration of the inhibitor for 1 hour and then the samples are dried. This is mounted directly on the specimen metal disc using adhesive tape. Samples are scanned at various scan areas using VEGA3TESCAN scanning

electron microscope. Digital images are stored in computer and processed.

2.4 Energy Dispersive X-ray analysis

VEGA3TESCAN scanning electron microscope connected with energy dispersive X-ray analyser is used to determine the elements present on the metal surface. The stainless steel specimens of dimension $2\text{ cm} \times 1\text{ cm} \times 0.04\text{ cm}$ are suspended in the best concentration of the inhibitor for 1 hour and then removed and dried and used for the analysis. From the peak intensity, percentage compositions of the elements are determined.

3. Results and Discussion

3.1 Weight loss method

Corrosion rates (CR) of the stainless steel immersed in 1 M HCl at various temperatures in the presence and absence of various concentrations of L-Glutamic acid (LG) and the inhibition efficiencies (IE) using mass loss method are calculated and the results are given in Table 3.1.

Table 3.1

The percentage inhibition efficiency and corrosion rate of corrosion of stainless steel in 1 M HCl by L-Glutamic acid (LG) at 303, 313 and 323 K by weight loss method

[LG] mM	Corrosion Rate $\times 10^{-2}$ $\text{gcm}^{-2}\text{h}^{-1}$			θ			% Inhibition Efficiency		
	303 K	313 K	323 K	303 K	313 K	323 K	303 K	313 K	323 K
0	4.795	8.333	18.636	-	-	-	-	-	-
0.68	2.334	-	-	0.51	-	-	51	-	-
1.4	2.188	-	-	0.54	-	-	54	-	-
2.0	2.151	-	-	0.55	-	-	55	-	-
2.7	2.078	-	-	0.56	-	-	56	-	-
3.4	1.932	-	-	0.59	-	-	59	-	-
4.0	1.932	6.831	16.137	0.59	0.18	0.13	59	18	13
4.7	1.896	6.291	14.902	0.60	0.24	0.20	60	24	20
5.4	1.853	6.198	14.332	0.61	0.25	0.23	61	25	23
6.1	1.750	5.315	13.347	0.63	0.36	0.28	63	36	28
6.8	1.714	4.723	12.800	0.64	0.43	0.31	64	43	31

The results show that the corrosion rate decreases on the addition of LG. This may be due to the adsorption of LG on the surface of the stainless steel through the interaction of N and O atoms present in LG with the stainless steel surface. Corrosion inhibition is strengthened with increase in the concentration of inhibitors. This trend results from the increased adsorption of LG on the surface of the metal. As a result the metal surface is effectively separated from the acid medium. Inhibition efficiency is found to decrease with increase in experimental temperature. This is an indication that at higher temperatures there might be desorption of LG from stainless steel surface. Decrease in inhibition efficiency with increase in temperature is an indication that the adsorption of LG on stainless steel surface is physical in nature [7-11].

3.2 Study of Kinetic and Thermodynamic Parameters on the Corrosion process

The relation between the corrosion rates (CR) and temperature (T) is expressed by the Arrhenius equation [12].

A plot of log of corrosion rate versus $1/T$ gives straight line and is shown in Figure 3.1. A plot of $\log (CR/T)$ versus $1/T$ gives straight line and is shown in Figure 3.2. The values of apparent activation energy (E_a), ΔH^\ddagger , ΔS^\ddagger and ΔG^\ddagger obtained from Arrhenius plot and transition state theory plot are given in Table 3.2.

Figure 3.1

Arrhenius plot for stainless steel corrosion in 1 M HCl in the absence and presence of different concentrations of LG

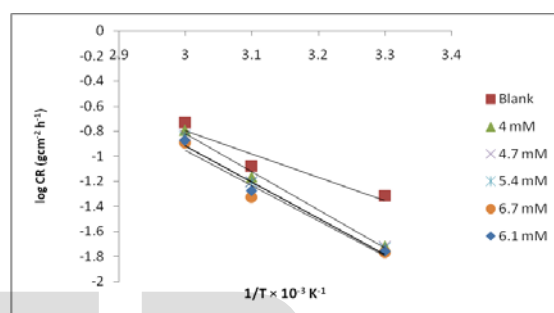


Figure 3.2

Transition state plot for stainless steel corrosion in 1 M HCl in the absence and presence of different concentrations of LG

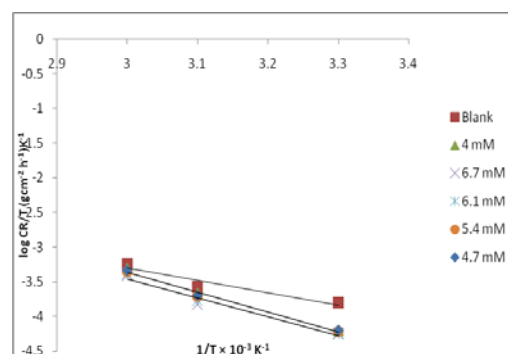


Table 3.2

Activation parameters of LG in 1 M HCl

[LG] mM	E _a (kJ mol ⁻¹)	ΔH [*] (kJ mol ⁻¹)	ΔS [*] (J mol ⁻¹ K ⁻¹)	ΔG [*] (kJ mol ⁻¹)		
				303 K	313 K	323 K
Blank	35.65	33.95	-159.44	82.26	83.85	85.45
4.7	56.10	54.38	-99.66	84.58	85.57	86.24
5.4	55.76	54.05	-100.95	84.64	85.65	86.66
6.1	54.86	53.15	-104.55	84.83	85.87	86.92
6.7	53.78	52.08	-108.39	84.92	86.01	87.08

Comparison of the activation energies at various concentration shows that the activation energy of the corrosion process increases on the addition of LG. The higher value of activation energy clearly reveals that the corrosion process is inhibited by the addition of inhibitor.

Experimental corrosion rate values evaluated from the weight loss data for stainless steel in 1 M HCl in the absence and presence of LG is used to determine the enthalpy of activation (ΔH^{*}) and apparent entropy of activation (ΔS^{*}) for the formation of the activated complex in the transition state using absolute reaction rate theory [13, 14]

The positive value of enthalpy of activation (ΔH^{*}) in the absence and presence of various concentration of inhibitor reflects the endothermic stainless steel dissolution process. Increase in the ΔH^{*} value with respect to the blank implies that the dissolution of stainless steel is difficult in the presence of inhibitor [15]. The value of ΔH^{*} is greater in the presence of the inhibitor than in the absence of inhibitor. This may be attributed to the higher energy barrier of the reaction, which

leads to rise in enthalpy of the corrosion process.

Entropy of activation of the corrosion process in free acid solution shows a large negative value. This implies that the transition state represents more orderly arrangement compared to the reactants.

The change in activation free energy (ΔG^{*}) of the corrosion process can be calculated at each temperature by applying the equation

$$\Delta G^* = \Delta H^* - T\Delta S^* \quad \dots(1)$$

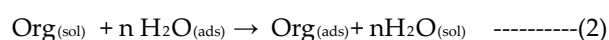
The increase in the ΔG^{*} value compared to the blank reveals that the formation of the activated corrosion complex becomes more difficult on the addition of inhibitor compared to the absence of inhibitor and hence the rate of corrosion decreases [16].

3.3 Adsorption isotherm

The effect of inhibitor concentration on the corrosion rate is quantified, generally, by fitting the surface coverage data, θ to equilibrium adsorption expressions, known as adsorption isotherm [17].

Adsorption isotherms provide important clues regarding the nature of metal- inhibitor interaction. In an effective adsorption of an inhibitor on metal surface, the force of interaction between metal and inhibitor is greater than the interactive force existing between metal surface and water molecules [18].

The adsorption of an organic adsorbate on to the metal solution interface is represented as a substitution process [19] between the organic molecules in the aqueous solution, Org_(sol) and the water molecules bound to the metallic surface, H₂O_(ads),



where $\text{Org}_{(\text{sol})}$ and $\text{Org}_{(\text{ads})}$ are the organic molecules in the aqueous solution and adsorbed on the metallic surface, respectively, $\text{H}_2\text{O}_{(\text{ads})}$ is the water molecules on the metallic surface and n is the size ratio representing the number of water molecules replaced from the metal surface by one molecule of organic adsorbent. When the equilibrium of the process described in this equation is reached, it is possible to obtain different expressions of the adsorption isotherm plot [20].

The inhibition of stainless steel corrosion in presence of various concentrations of LG has been attributed to their adsorption on the stainless steel surface, which is confirmed from the fit of the experimental data to various adsorption isotherms [21].

The θ values for different concentrations of inhibitors in 1 M HCl have been evaluated. The degree of surface coverage is found to increase with the increase in the concentration of the inhibitors and decreases as the temperature is raised from 303 K to 323 K. The data are fitted graphically to various adsorption isotherms such as the Langmuir, the Flory-Huggins and El-Awady et al.

3.3.1 Langmuir adsorption isotherm

In Langmuir adsorption isotherm, the surface coverage θ is related with the inhibitor concentration C .

C/θ is plotted against C at temperatures 303, 313 and 323 K and is shown in Figure 3.3.

Although the Langmuir plot is linear at room temperature with R^2 value closer to unity it does not obey Langmuir adsorption isotherm at higher temperatures which is evident from the negative slope value at higher temperatures [22, 23].

3.3.2 El-Awady et al adsorption isotherm

In El-Awady's adsorption isotherm, $\log(\theta/(1-\theta))$ is plot-

ted against $\log C$ and is shown in Figure 3.4. The adsorption parameters calculated from the El-Awady et al adsorption isotherm at three different temperatures are given in the Table 3.3. The R^2 values at all temperatures are close to unity. $K_{\text{ads}} = K^{1/y}$, K_{ads} is the equilibrium constant of the adsorption process and $1/y$ represents the number of active sites of the metal surface occupied by one molecule of LG. The values of $1/y$ and K_{ads} are calculated from the El-Awady et al model. The values of $1/y$ obtained are more than unity, indicating that the inhibitor LG is attached to more than one active site on the stainless steel surface [24]. However at higher temperatures $1/y$ is less than one. This clearly shows that at higher temperature desorption process occurs predominantly [25].

3.3.3 Flory-Huggins adsorption isotherm

The Flory-Huggins adsorption isotherm relates size parameter x and θ .

The plot of $\log(1-\theta)$ versus $\log \theta/C$ for the corrosion of stainless steel in 1 M HCl containing different concentrations of LG at various temperatures are shown in Figure 3.5. The Flory-Huggins adsorption isotherm parameters are calculated and the values are given in the Table 3.4.

The result shows that values for x are more than unity at 303 K, indicating that each molecule of inhibitor is attached to more than one active site on stainless steel surface [26-28]. At 303 K this isotherm fits well, but at higher temperature this is not the best fit. The R^2 value is 0.916 at 303 K. Thus the adsorption process is best explained by El-Awady et al adsorption isotherm.

The decrease in K_{ads} value with increase in temperatures in the El-Awady et al adsorption isotherm suggests that the inhibitors are physically adsorbed on the metal surface. The free energy of adsorption for the corrosion process in the absence

and presence of inhibitor are evaluated from the following equation

$$\Delta G^0_{\text{ads}} = -2.303 RT \log (55.55 \times K_{\text{ads}}) \quad \dots(3)$$

where ΔG^0_{ads} is Gibbs free energy of adsorption process, T is the temperature in Kelvin and K_{ads} is the equilibrium constant for the adsorption process and 55.55 is the molar concentration of water in solution. From the K_{ads} value obtained from El-Awady et al adsorption isotherm ΔG^0_{ads} is calculated. The negative value of ΔG^0_{ads} indicates that the adsorption process is spontaneous. Decrease in the value of K_{ads} at various temperatures implies physical adsorption. The ΔG^0_{ads} value which is closer to -20 kJmol^{-1} suggests that it is physical adsorption.

Assuming the thermodynamic model, corrosion inhibition of stainless steel in the presence of LG can be better explained using the enthalpy of adsorption (ΔH^0_{ads}) and entropy of adsorption (ΔS^0_{ads}) which can be calculated from the integrated van't Hoff equation [29]

To calculate the enthalpy of adsorption (ΔH^0_{ads}) and entropy of adsorption (ΔS^0_{ads}), the $\ln K_{\text{ads}}$ is plotted against $1/T$ (Figure 3.6a) and a straight line is obtained with a slope equal to $(\Delta H^0_{\text{ads}}/R)$ and intercept equal to $(\Delta S^0_{\text{ads}}/R + \ln 1/55.55)$.

The enthalpy of adsorption can also be calculated from the Gibbs-Helmholtz equation [30]

The variation of $\Delta G^0_{\text{ads}}/T$ versus $1/T$ gives a straight line with a slope equal to ΔH^0_{ads} (Figure 3.6b). It can be seen from the figure that the value of $\Delta G^0_{\text{ads}}/T$ decreases with $1/T$ linearly.

The calculated values of the heat of adsorption and entropy of adsorption using van't Hoff equation and Gibbs-Helmholtz equations are given in Table 3.5.

The negative value of the ΔH^0_{ads} indicates that the adsorption

of LG molecules is an exothermic process. If the value of ΔH^0_{ads} is less than or around -40 kJmol^{-1} the adsorption process is physisorption while if the value is more than -100 kJ mol^{-1} the adsorption of inhibitor follows chemisorption process [30]. According to El-Awady et al. adsorption isotherm the value is around -98 kJmol^{-1} . The molecules are adsorbed on metal surface by both physical and chemical adsorption. The negative value of ΔS^0_{ads} indicates that the adsorption phenomenon is a spontaneous process [31].

Figure 3.3

Langmuir adsorption isotherm plot for corrosion of stainless steel in 1 M HCl containing different concentrations of LG at 303, 313 and 323K

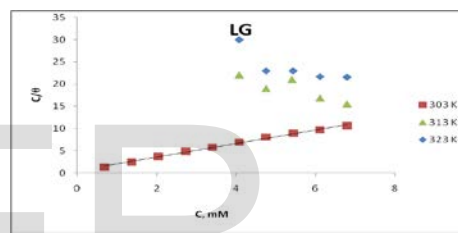


Figure 3.4

El-Awady et al adsorption isotherm plot for corrosion of stainless steel in 1 M HCl containing different concentrations of LG at 303, 313 and 323K

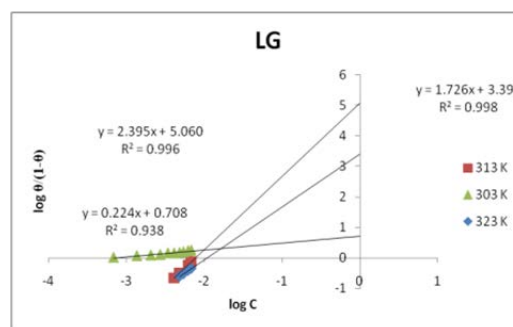


Table 3.3

Adsorption parameters calculated from El-Awady et al adsorption isotherm for LG

Inhibitor	R^2		$1/y$	$K_{ads} M^{-1}$	$\Delta G^0_{ads} kJ mol^{-1}$
LG	303 K	0.938	4.464	1447	-28.46
	313 K	0.996	0.579	850	-28.01
	323 K	0.998	0.417	26	-19.55

Figure 3.5

Flory Huggins adsorption isotherm for corrosion of stainless steel in 1 M HCl containing different concentrations of LG at 303, 313 and 323 K

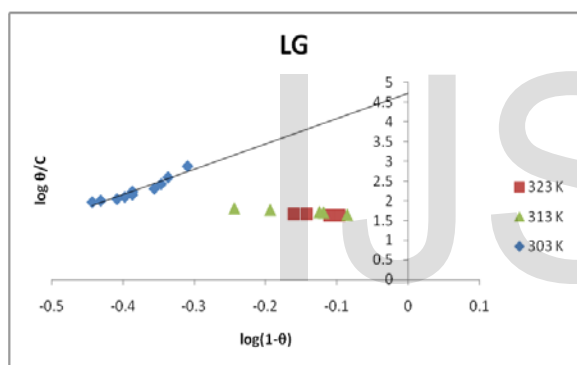


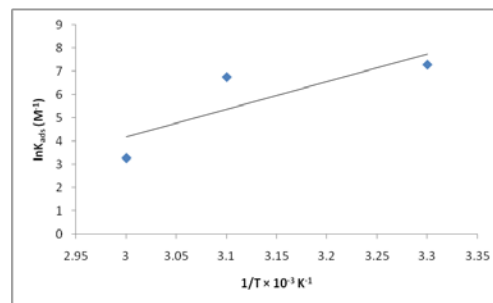
Table 3.4

Adsorption parameters calculated from Flory-Huggins adsorption isotherm for LG

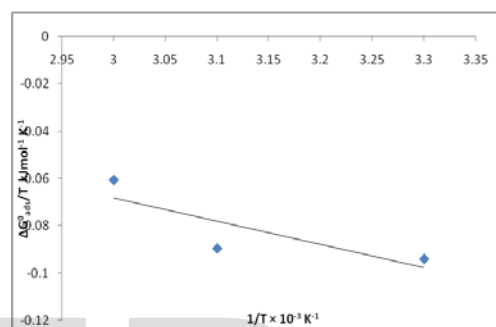
Inhibitor	R^2		X	$K_{ads} M^{-1}$	$\Delta G^0_{ads} kJ mol^{-1}$
LG	303 K	0.916	5.327	6.4	-14.79

Figure 3.6

and $1/T$ from El-Awady et al adsorption isotherm



(a)



(b)

Table 3.5

Heat of adsorption and entropy of adsorption values calculated from different thermodynamic equations

Different thermodynamic equations		$\Delta H^0_{ads} (kJ mol^{-1})$	$\Delta S^0_{ads} (J mol^{-1} K^{-1})$
van't Hoff Equation	El-Awady et al	-98.60	-32.94
Gibbs-Helmholtz Equation	El-Awady et al	-98	

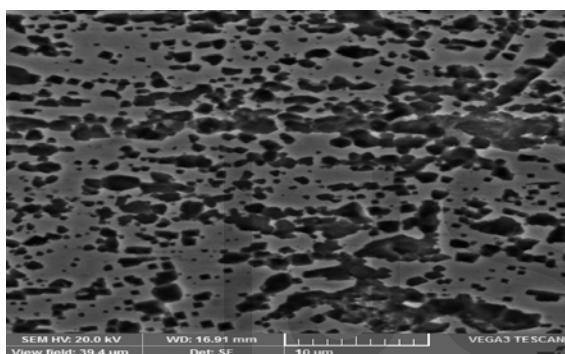
3.4 Scanning Electron Microscopy analysis

a) The relation between $\ln K_{ads}$ and $1/T$ from El-Awady et al adsorption isotherm b) The relationship between $\Delta G^0_{ads}/T$

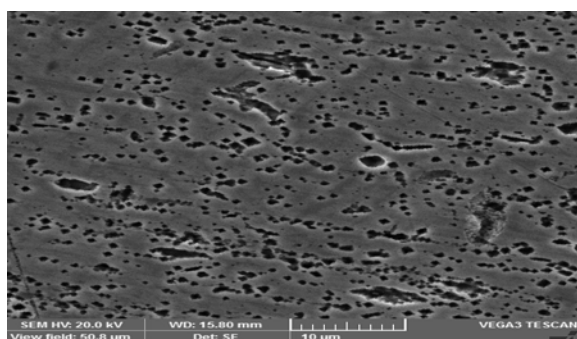
Scanning electron microscopy photographs obtained for stainless steel surface after immersion in 1 M solution for 1 hour in the absence and presence of 6 mM LG are shown in Figure 3.7. The stainless steel surface is greatly corroded in HCl solution in the absence of LG (Figure 3.7a). On the other hand, it is observed that the addition of inhibitor results in the formation of a protective layer on the surface which greatly reduces corrosion. Smoothness of the surface has been improved [32, 33] (Figure 3.7b).

Figure 3.7

SEM image of stainless steel after 1 hour immersion in (a) 1 M HCl (b) 1 M HCl containing 6 mM LG



(a)



(b)

3.5 Energy Dispersive X-ray analysis

EDX spectroscopy is used to determine the elements present on the stainless steel surface before and after exposure to the inhibitor solution. Figure.3.8 (a&b) presents the EDX spectra for stainless steel and stainless steel in the presence of optimum concentration of LG. The elemental compositions of stainless steel and stainless steel in 1 M with inhibitor are given in the Table 3.6.

In the presence of the optimum concentration of the inhibitor, oxygen, carbon and nitrogen are found to be present on the stainless steel surface. This indicates that the inhibitor molecules are adsorbed on the stainless steel surface and hence protects the stainless steel surface against corrosion [34-36].

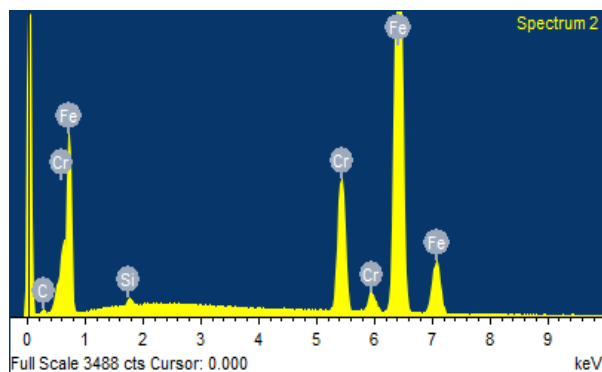
Table 3.6

Elemental composition of stainless steel surface and after immersion in 1 M with inhibitor for 1 hour

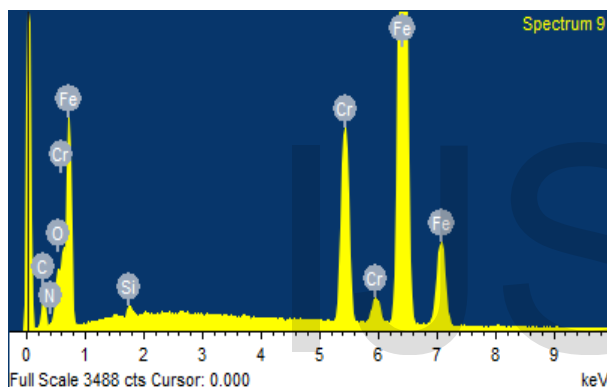
System	Atomic percentage				
	Fe	Cr	C	O	N
Stainless steel	73.8	15.79	9.65	-	-
Stainless steel + 1 M HCl + Inhibitor	53.3 7	10.93	27.47	7.32	0.3 3

Figure 3. 8

(a) EDX spectra of stainless steel surface (b) EDX spectra of stainless steel specimen after immersion in 1 M HCl with 6 mM LG



(a)



3.6 Quantum Chemical studies

Theoretical studies support the experimental results and therefore, in recent days corrosion inhibition studies include substantial quantum chemical calculations [37]. Quantum chemical calculations are performed with complete geometry optimizations using standard Gaussian-09 software package [38]. Calculations are done using the DFT/B3LYP combination to estimate molecular properties that are related to molecular reactivity. The use of the 6-31G (d, p) is meant to investigate the influence of addition of diffused orbitals on the calculated molecular parameters. The molecular properties that are well reproduced by density functional theory (DFT/B3LYP), include the energy of the highest occupied molecular orbital (HOMO) and energy of the lowest unoccupied molecular or-

bital (LUMO). They also include electronegativity, global hardness, global softness, electron affinity, ionization potential and dipole moment. These quantities are often defined following Koopman's theorem [39]. Electronegativity (χ) is the measure of the power of an electron or group of atoms to attract electrons towards itself [40] and according to Koopman's theorem; it can be estimated using the following equation

$$\chi \cong -1/2(E_{\text{HOMO}} - E_{\text{LUMO}}) \quad \dots(4)$$

where E_{HOMO} is the energies of the highest occupied molecular orbital and E_{LUMO} is the energy of the lowest unoccupied molecular orbital.

Global hardness (η) measures the resistance of an atom to a charge transfer [41] and it is estimated using the equation:

$$\eta \cong -1/2(E_{\text{HOMO}} - E_{\text{LUMO}}) \quad \dots(5)$$

Global softness (σ) describes the capacity of an atom or group of atoms to receive electrons [42] and the value is estimated with the equation:

$$\sigma = 1/\eta \cong -2 / (E_{\text{HOMO}} - E_{\text{LUMO}}) \quad \dots(6)$$

where η is the global hardness value

Electron affinity (EA) is related to E_{LUMO} through the equation:

$$EA \cong - E_{\text{LUMO}} \quad \dots(7)$$

Ionization potential (IP) is related to the E_{HOMO} through the equation:

$$IP \cong - E_{\text{HOMO}} \quad \dots(8)$$

The change in the number of electrons transferred is estimated by the equation

$$\Delta N = \chi_{\text{Fe}} - \chi_{\text{inh}} / 2(\eta_{\text{Fe}} - \eta_{\text{inh}}) \quad \dots(9)$$

where χ_{Fe} and χ_{inh} denote the absolute electronegativity of iron and the inhibitor molecule respectively; η_{Fe} and η_{inh} denote the absolute hardness of iron and the inhibitor molecule respectively. The values of χ_{Fe} and η_{Fe} are taken as 7eVmol⁻¹ and 0eVmol⁻¹ respectively [43].

Molecular properties of the inhibitors provide information on their activity. The selected molecular properties include the E_{HOMO} , the E_{LUMO} , the energy difference between the HOMO and the LUMO (ΔE), the dipole moment, μ , the number of electrons transferred (ΔN) from the inhibitor molecule to the metal atom global hardness, η and electronegativity, χ of the inhibitor. The calculated values of LG are given in Table 3.7. The geometry optimized structure, the highest occupied molecular orbital and the lowest unoccupied molecular orbital of LG (B3LYP/6-31G (d,p) results) is shown in Figure 3.9

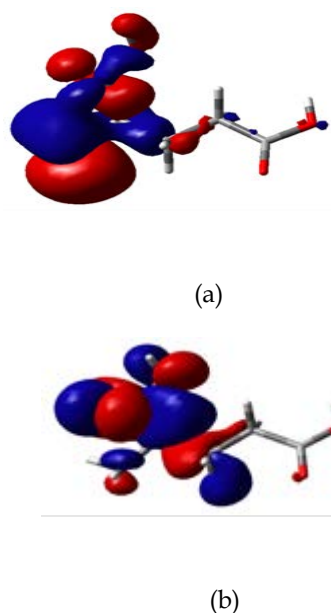
Table 3.7

Quantum chemical parameters for LG calculated using B3LYP/6-31G (d, p)

S.No.	Quantum chemical parameters	Values
1	Total energy(au)	-551.60797005
2	E_{HOMO} (eV)	-0.25507
3	E_{LUMO} (eV)	-0.006603
4	ΔE (eV)	0.2484
5	Fraction of electron transfer ΔN	28.70
6	Dipole moment (μ)(D)	5.0875
7	Ionisation potential(I) (eV)	0.25507
8	Electron affinity(A) (eV)	0.006603
9	Electron negativity(χ)(eV)	0.1308
10	Chemical hardness (η)	0.1242
11	Chemical softness (σ)	8.0482

Figure 3.9

The highest occupied molecular orbital and the lowest unoccupied molecular orbital of LG (B3LYP/6-31G (d, p) results)



The E_{HOMO} value of LG is -0.25507. Higher the E_{HOMO} , greater is the tendency of a molecule to donate its electrons to the electron poor species and therefore a comparison of the E_{HOMO} of the studied inhibitor molecule provides information about the tendency of the molecule to donate electron to the metal. Lower the E_{LUMO} , greater is the tendency of a molecule to accept electrons from an electron rich species.

The energy difference (ΔE) between HOMO and LUMO provides information about the overall reactivity of the molecules. The ΔE value of LG is 0.2484 eV. This shows the reactivity of the molecule. The dipole moment, μ , provides information on the polarity of the molecule and it is also a good reactivity indicator. The dipole moment has been reported to increase with increase in the inhibition efficiency of the inhibitor [44]. The dipole moment has also been reported to decrease with the increase in the inhibition efficiency of the inhibitor. Literature works show that the dipole moment does not correlate well with the corrosion inhibition efficiency [45]. The number of electron transferred (ΔN) indicates the tendency of a molecule to donate electrons to the electron poor species. If $\Delta N < 3.6$, the inhibition efficiency increases by increasing electron-

donating ability of these inhibitors to donate electrons to the electron poor species. The ΔN value of LG is 28.70; a higher value of ΔN implies a greater tendency to interact with the metal surface, that is, a greater tendency to donate electrons to the metal surface. The positive value of ΔN implies that the interaction between the inhibitor and the metal surface involves electron transfer. The higher E_{HOMO} value, higher ΔN value and lower ΔE value of LG implies that it provides better inhibition efficiency [46-49].

4. Conclusion

The experimental results reveal that inhibition efficiency increases with increase in inhibitor concentration. The maximum efficiency obtained for LG at room temperature is 64%.

The inhibition efficiency of LG decreases with increase in the temperature.

The higher energy of activation value in the presence of adsorbed molecules the metal dissolution takes up different path for which activation energy is high. The positive value of enthalpy of activation (ΔH^*) indicates that corrosion of metal in acid is an exothermic process. The negative value apparent entropy of activation (ΔS^*) shows that the transition state has more orderly arrangement than the reactants.

The adsorption of LG on stainless steel follows the El-Awady et al adsorption isotherm model. The free energy of adsorption (ΔG^0_{ads}) suggests that adsorption is a spontaneous physisorption process.

SEM and EDX analysis confirm the formation of protective film on the metal surface.

The quantum chemical parameters show a good correlation between the experimentally calculated inhibition efficiency and theoretical inhibition efficiency.

5. Reference

[1] Mwadham M. Kabanda, Ime B. Obot, Eno E. Ebenso, Computational Study of Some Amino Acid Derivatives as Potential Corrosion Inhibitors for Different Metal Surfaces and in Different Media, *Int.J.Electrochem.Sci.*, vol.8, pp-10839-10850, 2013.

[2] K. Barouni, L.Bazzi, R. Salghi, M. Mihit, B. Hammouti, A.Albourine and S.El Issami, Some Amino acids as corrosion inhibitors for copper in nitric acid solution, *Materials Letters*, vol.62, 19, pp. 3325-3327, July 2008.

[3] K. Barouni, A.Kassale, A. Albourine, O. Jbara, B. Hammouti and L.Bazzi, Amino acids as corrosion inhibitors for copper in nitric acid medium Experimental and theoretical study, *J. Mater.EnvIRON.Sci.*, vol. 5, issue- 2, pp. 456-463, 2014.

[4] Ingrid Milosev, Jasminka Pavlinac, Milan Hodoscek and Antonija lesar, Amino acids as corrosion inhibitors for copper in acidic medium: Experimental and theoretical study, *J.Serb. Chem.Soc.*, vol. 78, issue. 12, pp. 2069-2086, 2013.

[5] K.Barouni, M. Mihit, L.Bazzi,R.Salghi, S.S. Al-Deyab, B.Hammouti and A.Albourine, The inhibited Effect of Cysteine towards the corrosion of copper in nitric acid solution, *The open Corrosion Journal*, vol. 3, pp. 58-63, 2010.

[6] K. Barouni, A. Kassale, L. Bazzi, R.Salghi, B. Hammouti, A.Albourine, S.El Issami and O.Jbara, inhibition of Corrosion of copper in nitric acid solution by four amino acids, *Research on Chemical Intermediates*, vol.40, issue.3, pp. 991-1002, 2014.

[7] P. Angel, A. Sahaya Raja, J. Sathiyabama and V. Prathipa, Corrosion inhibition of vitexnegundo extract as a green corrosion inhibitor for carbon steel in well water, *International Journal of Chemical studies*, vol.2 issue.1, 2014.

[8] A.S. Fouda, G.Y.Elewady, K. Shalabi and S. Habbouba, Gibberellic acid as green corrosion inhibitor for carbon steel in hydrochloric acid solutions, *J. Mater. Environ.Sci.*, vol.5, issue.3, pp.767-778, 2014.

[9] T. Kasilingam and C.Thangavelu, Nano analyses of protective film on to carbon steel, *International journal of innovative technology and exploring engineering*, vol. 3, issue.12, 2014.

[10]C. Mary Anbarasi, M. Alagumani and K. Sowmiya, Electrochemical and surface analysis studies on corrosion inhibition of carbon steel by octanesulphonic acid- Ni^{2+} system, *Applied Sciecnas, Engineering and Technology*, pp.27-29, 2014.

[11] Vijaya Gopal sribharathy and Susai Rajendran, Corrosion inhibition of Carbon steel by sodium metavanadate, *J. Electrochem. Sci.*, vol. 2, 2012.

[12] A. Popova, E. Sokolova, S. Raicheva and M. Christov, AC and DC study of the temperature effect on mild steel corrosion in acid media in the presence of benzimidazole derivatives, *Corrosion Science*, vol.45, issue.1, pp.33-58, 2003.

[13] I. Hamdani, E.El Ouariachi, O. Mokhtari, A. Salhi, N. Chahboun, B. ElMahi, A. Bouyanzer, A. Zarrouk, B. Hammouti and J. Costa, Chemical constituents and corrosion inhibition of mild steel by the essential oil of *Thymus algeriensis*

in 1.0 M hydrochloric acid solution, *Der pharma Chemica*, vol. 7, issue.8, pp.252-264, 2015.

[14] E.E.Oguzie, Corrosion inhibition of aluminium in acidic and alkaline media by Sansevieria trifasciata extract, *Corrosion Science.*, vol.49, issue. 3, pp.1527-1539, 2007.

[15] L.R. Chauhan, G. Gunasekaran, Corrosion inhibition of mild steel by plant extract in dilute HCl medium, *Corrosion Science.*, vol.49, issue.3, pp.1143-1161, 2007.

[16] H. Ashassi-Sorkhabi, B. Shaabani and D. Seifzadeh, Corrosion inhibition of mild steel by some Schiff base compounds in hydrochloric acid, *Applied surface science.*, vol. 239, issue.2, pp.154-164, 2005.

[17] Sudhish kumar shukla and M.A. Quraishi, Cefotaxime sodium: a new and efficient corrosion inhibitor for mild steel in hydrochloric acid solution, *Corrosion Science*, vol.51, issue.5, pp.1007-1011, 2009.

[18] M.Sahin, S. Bilgic and H.Yilmaz, The inhibition effects of some cyclic nitrogen compounds on the corrosion of the steel in NaCl mediums, *Applied Surface Science.*, vol.195, issue.1-4, pp.1-7, 2002.

[19] K.F. Khaled, Experimental and theoretical study for corrosion inhibition of mild steel in hydrochloric acid solution by some new hydrazine carbodithioic acid derivatives, *Applied Surface Science.*, vol.252, issue.12, pp.4120-4128, 2006.

[20] Y.X. Hua and Q.B. Zhang, Corrosion inhibition of mild steel by alkylimidazolium ionic liquids in hydrochloric acid, *Electrochimica acta*, vol.54, issue.6, pp.1881-1887, 2009.

[21] A.Y. El-Etre, M. Abdallah and Z.E. El-Tantawy, Corrosion inhibition of some metals using lawsonia extract, *Corrosion Science.*, vol.47, issue.2, pp.385-395, 2005.

[22] R.Karthikaselvi and S. Subhashini, Study of adsorption properties and inhibition of mild steel corrosion in hydrochloric acid media by water soluble composite poly (vinyl alcohol-o-methoxy aniline), *Journal of the Association of Arab Universities for Basic and Applied Sciences*, vol. 16, pp.74-82, 2014.

[23] Nour Sh. El-Gendy and A. Hamdy, Thermodynamic, adsorption and electrochemical studies for corrosion inhibition of carbon steel by henna extract in acid medium, *Egyptian Journal of Petroleum*, vol.22, issue.1, pp.17-25, 2013.

[24] E.E. Foad El Sherbini, Sulphamethoxazole as an effective inhibitor for the corrosion of mild steel in 1.0 M HCl solution, *Materials Chemistry and Physics*, vol.6, issue.1(3), pp. 223-228, 1999.

[25] M. Sahin, G. Gece, F. Karci and S. Bilgic, Experimental and theoretical study of the effect of some heterocyclic compounds on the corrosion of low carbon steel in 3.5% NaCl medium.,

Journal of applied electrochemistry, vol.38, issue.6, pp.809-815, 2008.

[26] Ashish K. Singh, Sudhish K.Shukla, M.A. Quraishi and Eno E. Ebenso, Investigation of adsorption characteristics of N,N'-I(methylimino)dimethylidyneldi-2,4-xylydine as corrosion inhibitor at mild steel/sulphuric acid interface, *Journal of the Taiwan institute of chemical Engineers*, vol.43, issue.3, pp.463-472, 2012.

[27] E. Samiento-Bustos, J.G. Gonzalez, J. Uruchurtu, G. Dominguez-Patino and V.M. Salinas-Bravo, Effect of inorganic inhibitors on the corrosion behaviour of 1018 carbon steel in the LiBr+ethylene glycol+H₂O mixture, *Corrosion Science*, vol.50, issue.8, pp.2296-2303, 2008.

[28] Ayse Ongun Yuce and Gulfeza Kardas, Adsorption and inhibition effect of 2-thiohydantoin on mild steel corrosion in 0.1 M HCl, *Corrosion Science*, vol.58, pp.86-94, 2012.

[29] Tianpei Zhao and Guannan Mu, The adsorption and corrosion inhibition of anion surfactants on aluminium surface in hydrochloric acid, *Corrosion Science*, vol.4, issue.10, pp.1937-1944, 1999.

[30] Ehteram A. Noor and Aisha H. Moubaraki, Thermodynamic study of metal corrosion and inhibitor adsorption processes in mild steel/1-methyl-4-(X)-styrylpyridinium iodides/hydrochloric acid systems, *Materials Chemistry and Physics*, vol.110, pp.145-154, 2008.

[31] Ansari, M. Znini, A. Laghchimi, J. Costa, P. Ponthiaux and L. Majidi, Chemical composition, adsorption properties and corrosion inhibition on mild steel of Mentha rotundifolia L. essential oil from Morocco, *Der Pharmacia Lettre*, vol.7, issue.6, pp.125-140, 2015.

[32] S.A.M. Refaey, F. Taha and A.M. Abd El-Malak, Corrosion and Inhibition of 316L stainless steel in neutral medium by 2-Mercaptobenzimidazole, *Int. J.Electrochem. Sci.*, vol.1, pp.80-91, 2006.

[33] Mahdi Nasibi, Milad Mohammady, Effat Ghasemi, Ali Ashrafi, Davood Zaarei and Gholamreza Rashed, Corrosion inhibition of mild steel by Nettle (Urtica dioica L.) extract: polarization, EIS, AFM, SEM and EDS studies, *Journal of Adhesion Science and Technology*, vol.27, issue.17, pp.1873-1885, 2013.

[34] E.M. Sherif and Su-Moon Park, Inhibition of copper corrosion in acidic pickling solutions by N-phenyl-1,4-phenylenediamine, *Electrochimica Acta*, vol.51, issue.22, pp.4665-4673, 2006.

[35] Khaled F. Khaled, Omar A. Hazzazi, Mohammed A. Amin and Khaled F. Khaled, On the corrosion inhibition of low carbon steel in concentrated sulphuric acid solutions. Part I: Chemical and electrochemical (AC and DC) studies, *Corrosion Science*, vol.50, issue.8, pp.2258-2271, 2008.

- [36] El-Sayed M. Sherif, Effects of 2-amino-5-(ethylthio)-1,3,4-thiadiazole on copper corrosion as a corrosion inhibitor in 3% NaCl solutions, *Applied Surface science*, vol.252, issue.24, pp.8615-8623, 2006.
- [37] Mwadham M Kabanda, Lutendo C. Murulana, Muzaffer Ozcan, Faruk Karadag, Faruk Karadag, Ilyas Dehri, I.B. Obot and Eno E. Ebenso, Quantum chemical studies on the corrosion inhibition of mild steel by some triazoles and Benzimidazole derivatives in acidic medium, *Int. J. Electrochem.Sci*, vol.7, pp.5035-5056, 2012.
- [38] Majid Khodaei-Tehrani and Ali Niazi, Quantum chemical studies on the corrosion inhibition of some heterocyclic bases on mild steel in acidic medium, *Oriental Journal of Chemistry*, vol.31, issue.1, 2010.
- [39] R.Banerjee, Ranjana, S S Panya and M M Nandi, An electrochemical and quantum chemical investigation of some inhibitors on Aluminium alloy in 0.6 M aqueous sodium chloride solution, *Indian journal of chemical Technology*, vol.18, pp.309-313, 2011.
- [40] P.Senet, Chemical hardness of atoms and molecules from frontier orbitals, *Chem.Phys.Lett*, vol.275, pp.527, 1997.
- [41] P.Geerlings, F. De Proft, W. Langenaeker, Conceptual Density Functional theory, *Chemical Review*, 103, 1793, 2003.
- [42] R.G. Parr, R.G. Pearson, Absolute hardness: companion parameter to absolute electronegativity, *J. Am.Chem. Soc.*, 105, 7512, 1983.
- [43] L. Pauling, The Nature of the chemical bond, *Coruelli University press, Ithaca, New York*, 1960.
- [44] Mahendra Yadav, Sushil Kumar, Indra Bahadur, Deresh Ramjugernath, Electrochemical and quantum chemical studies on synthesized phenylazopyrimidone dyes as corrosion inhibitors for Mild steel in a 15% HCl solution, *Int. J. Electrochem.Sci.*, vol.9, pp.3928-3950, 2014.
- [45] Mahendra Yadav, Sushil Kumar, Debasis Behera, Indra Bahadur, Deresh Ramjugernath, Electrochemical and quantum chemical studies on adsorption and corrosion inhibition performance of Quinoline-Thiazole derivatives on mild steel in hydrochloric acid solution, *Int.J.Electrochem.Sci*, vol.9, pp.5235-5257, 2014.
- [46] G. Raja, K. Saravanan and S.Sivakumar, Quantum chemical and corrosion inhibition studies of an organic compound: 2, 5 Dichloroaniline, *Rasayan journal*, vol. 8, issue .1, pp. 8-12, 2015.
- [47] W.Li, L. Hu, Z. Tao, H. Tian and B.Hou, Experimental and quantum chemical studies on two triazole derivatives as corrosion inhibitors for mild steel in acid media, *Materials and Corrosion*, vol. 62, issue.11, pp. 1042-1050, 2011.
- [48] Asan R Obayes, Ghadah H Alwan, Abdul Hameed M J Alodaidey, Ahmed A Al-Amiery, Abdul Amir H Kadhum and Abu Bakar Mohamad, Quantum chemical assessment of benzimidazole derivatives as corrosion inhibitors, *Chemistry Central Journal*, vol.8, pp.21, 2014.
- [49] Ameh P O, Koha P U and Eddy N O Experimental and quantum chemical studies on the corrosion inhibition potential of phthalic acid for mild steel in 0.1 M H₂SO₄, *Chem Sci J*, vol. 6, pp.3, 2015.